For submission to International Journal of Remote Sensing

Cloud Base Heights Retrieved During Nighttime Conditions with MODIS Data

Keith Hutchison[*], Eric Wong[#], and S. C. Ou[$]

ABSTRACT

The capability to retrieve cloud base heights was developed under the United States National Polar-orbiting Operational Environmental Satellite System (NPOESS) program as one of 27 data products to be created from data collected by the Visible Infrared Imager Radiometer Suite (VIIRS). First launch of the VIIRS sensor, which is the high-resolution Earth imager of the NPOESS program, comes on NASA's NPOESS Preparatory Project (NPP). In preparation for this launch, extensive testing of the VIIRS cloud algorithms was completed to verify product performance will satisfy system requirements before the cloud algorithms were hosted in the NPOESS ground processing center. The approach taken to retrieve cloud base height converts cloud optical properties into a geometric thickness which is then subtracted from the cloud top height. Performance of the cloud base height algorithms has been recently verified using MODIS data along with temporarily and spatial coincident observations of cloud thickness values made with the millimeter cloud radar operated by NOAA at the Mesonet facility in Oklahoma. Of particular significance is the clear demonstration that both cloud optical properties and cloud base heights are accurately retrieved during nighttime conditions with the VIIRS algorithms since neither of these products is currently produced by the NASA EOS program. Based upon these analyses, the VIIRS cloud algorithms are

expected to satisfy NPOESS requirements, making VIIRS the first operational satellite sensor capable of retrieving 3-dimensional cloud fields.

---

* Corresponding Author: Keith Hutchison, Center for Space Research (CSR), The University of Texas at Austin, 3925 W. Braker Lane, Ste. 200, Austin, TX 78759, keithh@csr.utexas.edu, (512)-471-7295

Eric Wong, Northrop Grumman Space Technology (NGST), NPOESS System Engineering, Modeling & Simulations, One Space Park, Redondo Beach, CA 90245

$ S. C. Ou, University of California, Los Angeles, Department of Atmospheric and Oceanic Sciences, 405 Hilgard Avenue, 7127 Math Sciences Bldg.
Los Angeles, CA 90095-1565

1.0 INTRODUCTION

The National Polar-orbiting Operational Environmental Satellite System (NPOESS) was established by Presidential Decision Directive NSTC-2 on May 5, 1994. This directive required the Departments of Commerce (DoC) and Defense (DoD), and NASA to create an Integrated Program Office (IPO) to develop, acquire, manage, and operate the next generation of polar-orbiting operational environmental satellites for the United States. The NPOESS IPO was established on October 3, 1994 with a mandate that extends to the year 2018. The IPO has partnered with the European Organisation for the Exploitation of Meteorological Satellites (EUMETSAT) and the National Space Development Agency of Japan (NASDA) to ensure a long-term continuity of observations from polar orbit will continue to support improvements in the operational meteorological, environmental, and climate monitoring services of its user communities.

NPOESS satellites will carry numerous sensors to collect data from the visible through the microwave regions of the electromagnetic spectrum that will be used to create a large number of data products, also called environmental data products. The Visible/Infrared Imager Radiometer Suite (VIIRS) is the NPOESS high-resolution Earth viewing sensor. VIIRS has its heritage in three sensors currently collecting imagery of the Earth, including NOAA's Advanced Very High Resolution Radiometer (AVHRR), NASA's MODerate Resolution Imaging Spectroradiometer (MODIS), and the DoD's Operational Linescan Sensor (OLS) flown by the Defense Meteorological Satellite Program (DMSP). Like MODIS, VIIRS will provide highly calibrated data in all channels collected using

four-focal plane assemblies. In addition, it relies heavily upon its MODIS and AVHRR heritage for spectral bandpass definitions used in automated cloud detection algorithms. VIIRS also relies upon its DMSP OLS heritage to provide data at edge of scan that grows to no more than twice its spatial resolution at nadir. VIIRS will collect data at two nominal resolutions at nadir: 375 m in "Imagery" channels and 750 m in "Radiometric" channels. Finally, VIIRS contains the legacy to the DMSP nighttime (low light) visible channel, known as the Day-Night Band (DNB). First launch of the VIIRS sensor comes on NASA's NPOESS Preparatory Project (NPP).

Data collected by the VIIRS sensor will be used to create nearly 30 environmental data products including cloud analyses, land and ocean surface products, and aerosol products. These products will be delivered to a diverse user community in the DoC, DoD, and at NASA that support applications from the real-time to long-term, climate change timescales and VIIRS has been designed to satisfy this full range of requirements.

The approach to retrieve cloud base height converts cloud optical properties into geometric thickness which is then subtracted from cloud top heights. Performance of the cloud base height algorithms, for both ice and water cloud top phase, has been recently verified using MODIS data along with temporarily and spatial coincident observations of cloud thickness values made with the millimeter cloud radar operated by NOAA at the Mesonet facility in Oklahoma. In this paper, it is clearly demonstrated that cloud optical properties, cloud top heights and cloud base heights are accurately retrieved during nighttime conditions with the VIIRS algorithms. Since neither of these data products is

currently produced by the NASA Earth Observing System program, the enhanced capability to retrieve cloud properties in nighttime data is considered to be of particular significance for the operational and climate change communities. Based upon these analyses, the VIIRS cloud algorithms are expected to satisfy NPOESS requirements, making VIIRS the first operational satellite sensor capable of retrieving 3-dimensional cloud fields.

2.0 VIIRS CLOUD BASE HEIGHT ALGORITHMS

Requirements have been levied upon the VIIRS Cloud Base Height algorithms as shown in Table 1, which is taken from the NPOESS System Specification, the document that defines acceptable performance for the total NPOESS system and each sub-system. These requirements establish a requirement of +/- 2 km for both ice and water clouds. This rather “loose” requirement most likely suggests the low expectations by the NPOESS IPO that a more accurate cloud base height could be retrieved from passive remote sensing techniques since requirements for other applications, e.g. air quality management, desire cloud fields at 20-70 mb accuracy to match inputs of chemical models (Jacobson, private communication). Thus, a goal of this paper is to demonstrate 3-dimensional cloud fields, i.e. cloud top heights and cloud base heights, with an accuracy within 10’s of meters rather than kilometers.

As previously noted, the VIIRS cloud base height algorithms for use with ice and water clouds convert cloud optical properties, i.e. cloud optical thickness and effective particle

size, into geometric thickness (Hutchison, 2002). This conversion is based upon parameterization between cloud ice/liquid water path and cloud optical properties (Liou, 1992). Cloud base height is then calculated by subtracting cloud thickness from the cloud top height product for each VIIRS pixel. Therefore, it is evident that the cloud base height algorithms require, as ancillary data, numerous cloud products and the architecture for creating these products is shown in Figure 1.

Figure 1 here.

In this figure, processes containing algorithms are shown in "white" text while products created from those algorithms appear as "black" text. For example, the algorithms that retrieve cloud optical properties (COP) produce the products: cloud optical thickness (COT), cloud effective particle size (CPS), and cloud top temperature (CTT). The input field for the cloud module is the calibrated, earth-located VIIRS sensor data records or the field of brightness temperatures and reflectances for thermal and solar bands respectively. A detailed overview of the VIIRS cloud mask algorithms has appeared in the literature (Hutchison et al., 2005). The cloud phase algorithm follows the description provided by Pavolonis and Heidinger (2004) and provides the capability of identifying pixels that contain both cirrus and water clouds in multiple layers, along with mixed phase clouds, ice clouds, and water clouds. Two different algorithmic approaches are used to retrieve CTT: one simultaneously retrieved COT, CPS, and CTT and will be described in detail below since it is used with ice during day and nighttime conditions along with water clouds in nighttime data. The other approach is found in the cloud top parameters algorithm process and uses COT and CPS along with a radiative transfer

program to retrieve CTT for optically-thin, water clouds but only during daytime conditions. Once CTT is retrieved, other cloud top fields (pressure and height) are obtained by interpolation with NCEP atmospheric profiles. A parallax correction is applied then clouds are grouped into reporting intervals of approximately 6 km, known as the horizontal cell size (HCS) and cloud cover (CC) fraction and cloud cover layers (CC/L) are reported. Finally, for each layer in the HCS, a cloud type is specified which is related to cloud liquid water concentration or ice water concentration that are needed by the cloud base height algorithms. Therefore, the CBH algorithms are last in the processing chain. The final step moves the cloud products from satellite-space to a gridded field for use by operational users.

2.1 VIIRS CLOUD BASE HEIGHT ALGORITHMS

The retrieval of cloud base height solely from MODIS or VIIRS data is calculated from the difference between cloud top height and cloud thickness, as shown in Equation 1, where the latter is derived from cloud optical properties, i.e. effective particle size and optical depth (Hutchison, 2002; Hutchison, 1998). There are two algorithms that differ slightly according to cloud top phase. The cloud optical properties are corrected for viewing geometry such that all measurements are for the nadir position, as shown in Figure 2.

For water clouds, cloud thickness (ΔZ) is based upon the relationship between liquid water path (LWP), in gm/m^2, and liquid water content (LWC), which is the integration of cloud size distribution over droplet size and has units of gm/m^3. Liquid water path has

been related to cloud optical depth or cloud optical thickness (τ) and cloud effective cloud particle size (r_{eff}) as shown in Equation 2 (Liou, 1992, Table 4.2).

$$Z_{cb} = Z_{ct} - (\Delta Z) = Z_{ct} - [LWP/LWC] \quad (1)$$

where: $LWP = \text{Liquid water path} = [2 \tau r_{eff}] / 3 \quad (2)$

LWC = Liquid water content

τ = cloud optical depth

r_{eff} = cloud droplet effective particle size

Measurements show the value of the liquid water content varies between about 0.20 - 0.45 g/m^3, as a function of cloud type. Initially, the liquid water content is assumed constant throughout the vertical extend of the cloud. This assumption becomes increasingly less reliable as clouds become more thick (Slingo, 1982; Martin et al., 1994).

Figure 2 here.

The form of the cloud base height algorithm for ice clouds follows that for water clouds with the exception that the relevant terms in Equation 1 become Ice Water Path (IWP) and Ice Water Content (IWC) as shown in Equation 3. The parameterization for ice water path, shown in Equation 4 (Liou, 1992), is a function of cloud optical depth (τ), through the ice crystal size distribution, and ice crystal diameter ($D_e=2r_{eff}$).

$$Z_{cb} = Z_{ct} - (\Delta Z) = Z_{ct} - [IWP/IWC] \quad (3)$$

$$\text{where} \quad IWP = \tau / [a+b/D_e] \quad (4)$$

The regression coefficients (a) and (b) in Equation (4) are given by Liou (Table 5.4, 1992) with values a = - 6.656e-3; b = 3.686. The ice water content is a function of cloud top temperature and is given by:

$$\ln(IWC) = - 7.6 + 4 \exp[-0.2443e\text{-}3(|T| - 20)^{2.455}] \quad \text{for } |T| > 20 \text{ deg C} \tag{5}$$

Additionally, D_e is a function of cloud top temperature as shown by Ou et. al. (1993)

$$D_e = c_0 + c_1 T + c_2 T^2 + c_3 T^3 \tag{6}$$

where

$$c_0 = 326.3,\ c_1 = 12.42,\ c_2 = 0.197,\ c_3 = 0.0012 \tag{7}$$

Since the VIIRS CBH algorithms rely heavy upon the VIIRS COP EDRs and since the VIIRS COP algorithms are different from those used by MODIS which does not retrieve COP products during nighttime conditions, a more in-depth examination of these algorithms is pertinent.

2.2 VIIRS CLOUD OPTICAL PROPERTY ALGORITHMS

The VIIRS daytime solar algorithm follows that described in the literature (Nakajima and King, 1990; Platnick et al., 2003, Ou et al. 2003) with the exception that VIIRS uses look up tables exclusively while the MODIS approach applies asymptotic theory of optically thick layers to retrieve cloud properties with optical thickness values exceed about 12. The algorithm theoretical basis and performance of the MODIS daytime algorithms are well documented (King et al., 2003). VIIRS has no equivalent to MODIS Channels 33-36, which sample across the 13-14 μm band and are used with the CO_2 slicing algorithm approach to retrieve cloud top pressures of cirrus clouds, Therefore, VIIRS has a second algorithm, as shown in Figure 3, that is used to retrieve cloud top temperatures for cirrus clouds based upon the physical relaxation methodology described by Ou et al., (1993). This approach uses radiance data from AVHRR 3.7 μm and 10.9 μm channels to

simultaneously retrieve cirrus cloud top temperature, cloud optical depth, and cloud effective ice crystal size, based on the theory of radiative transfer and cloud parameterizations. This algorithm is presented in detail since it is used in the retrieval of COP for cirrus clouds under all solar illumination conditions and in the retrieval of COP with nighttime water clouds.

Figure 3 here.

The top of the atmosphere radiance (R_i) for the 3.7 μm and 10.76 μm channels, denoted for convenience as Channel 1 and Channel 2 respectively, over a cirrus cloudy atmosphere is described in terms of the cirrus cloud-top temperature T_c and emissivities (ε_1, ε_2) of each channel as follows:

$$R_i = (1 - \varepsilon_i) R_{ai} + \varepsilon_i B_i(T_c) \qquad \text{for } i = 1, 2 \tag{7}$$

where R_{ai} denotes the upwelling radiance reaching the cloud base and $B_i(T_c)$ is the respective Planck functions for the cloud top temperature. The first term on the right-hand side of Equation 7 represents the contribution of the transmitted radiance from below the cloud while the second term is the emission contribution from the cloud. Energy due to water vapor emission above the cirrus cloud is neglected as well as the effects of cloud reflectivity, these are generally less than 3 percent of the incident radiance. However, these emissions are considered in the analysis of water clouds.

To solve Equation 7 for T_c and ε_i numerically, ε_1 and ε_2 must be correlated and $B_1(T_c)$ is expressed in terms of $B_2(T_c)$. The clear-sky radiances R_{a1} and R_{a2} must also be known. First, to express $B_1(T_c)$ in terms of $B_2(T_c)$ the Planck functions are computed at 0.1 K intervals over the range of 150-300K while taking into account the respective channel filter functions. Values in the look up table are then fitted to a third-degree polynomial based on a least-square regression technique, where the regression coefficients for AVHRR were determined to be: a_0 = 2.6327e-4, a_1 = -1.063e-4, a_2 = 8.2976e-6, and a_3 = 3.7311e-7.

$$B_1(Tc) = \sum a_n[B_2(T_c)]^n = f[B_2(T_c)] \quad n = 0,1,2,3 \qquad (8)$$

Next, the relationship between the emissivities for the two channels is evaluated. The cirrus emissivities at the 3.7 μm and 10.76 μm wavelengths may be parameterized in terms of visible optical depths τ using the form:

$$\varepsilon_i = 1 - \exp(-k_i\tau) \quad \text{for } i=1,2 \qquad (9)$$

The exponential term represents the effective transmissivity where the parameters k_i represent the effective extinction coefficients for the two channels, accounting for multiple scattering within cirrus clouds and for the difference between visible and IR extinction coefficients. Thus the products $k_i\tau$ may be considered as the effective optical depth that would yield the same emissivity values for the nonscattering conditions at the 3.7 μm and 10.76 μm wavelengths. Eliminating τ from Equation 9, results in the desired relationship between ε_1 and ε_2:

$$(1-\varepsilon_1)^{1/k1} = (1-\varepsilon_{i2})^{1/k2} \quad (10)$$

The substitution of (7) into (10) results in a nonlinear, algebraic equation with $B_2(Tc)$ as the key unknown as shown in Equation (11).

$$[(R_2 - B_2(T_c))/(Ra_2 - B_2(T_c))] - [(R_1 - f[B_2(T_c)])/(Ra_1 - f[B_2(T_c)])]^{k2/k1} = 0 \quad (11)$$

To close the system of equations, a relationship is needed between the ratio k_2/k_1 which can be expressed in terms of $1/D_e$ in the form:

$$k_2 / k_1 = \sum_{n=0}^{2} b_n D_e^{-n}, \quad (12)$$

where the coefficients b_n are determined from a second-order least square method using the radiance tables. On the other hand, based on a dimensional analysis, a relationship between *De*, T_c and τ can be derived:

$$D_e = c\{\tau/[\Delta z(\alpha + \beta/D_e)\langle IWC\rangle]\}^{1/3}\langle D_e\rangle. \quad (13)$$

where Δz is the cloud thickness, and $\langle$*Ice Water Content (IWC)*$\rangle$ and $\langle D_e\rangle$ are the temperature dependent mean values of *IWC* and D_e, respectively:

$$\langle IWC\rangle = \exp\{-7.6 + 4\exp[-0.2443\times10^{-3}(253 - T_c)^{-2.445}]\}$$
For $T_c < 253$ K (14)

$$\langle D_e\rangle = \sum_{n=0}^{3} c_n (T_c - 273)^n \quad (15)$$

Thus, the procedure is as follows:

1. First, input VIIRS 3.7 μm and 10.76 μm radiance for cloudy pixels into the retrieval program
2. We then estimate mean cirrus cloud temperature and τ, k_2/k_1, and D_e for a retrieval domain through an optimization analyses. (See Equations 58-62 and Appendix B in VIIRS Cloud Optical Properties Algorithm Theoretical Basis Document, Ou et al 2002.) These are initial guess values.
3. Cloud top temperature is then calculated using Equation (11).
4. We subsequently evaluate τ, k_2/k_1, and D_e based on Equation (11), Equation (12), and Equation (13*)*
5. Finally, we put T_c, τ, and D_e to a convergence test, which checks whether the ratios of successively iterated cloud parameters are smaller than prescribed threshold values. If these parametric values are not converged, we repeat steps 3 and 4. If converged, then these parametric values are the solutions.

While the NPOESS program applies this retrieval approach to all cirrus clouds, during daytime and nighttime conditions as shown in Figure 3, the approach is consider more accurate with nighttime data. Results obtained by using this approach with daytime data could be impacted by the removal of the solar component of radiation from the 3.7 μm daytime data (Ou et al., 1995)), and by the fact that the 3.7 μm band senses a different part of the cloud from the two near-IR bands (1.6 and 2.25μm). Thus, during the daytime, the infrared retrieval approach is considered complementary to the solar method; however, the solar approach should be more reliable under most circumstances, except

possibly near local dawn and dusk, i.e. conditions found in the NPOESS terminator orbit. Once cloud optical thickness and effective particle size are retrieved with solar data, the 3.7 μm solar component is computed based on the solar retrieved cloud optical properties and is removed from the total radiance, and the same equations used in the IR technique are used to retrieve effective cloud top temperature.

Prior to NPOESS, no algorithm had been formulated to retrieve COP for water clouds in nighttime data. However, sensitivity studies demonstrated that this same approach could be applied to water clouds after corrections are made for differences in atmospheric transmittance between the two channels. Therefore, the retrieval of COP during nighttime conditions represent a higher risk that the daytime algorithms and become the focus of algorithm verification testing, as discussed in the next section.

3.0 TEST DATA SETS

The VIIRS CBH algorithms were used to analyze MODIS nighttime data collected of Oklahoma and performance established by comparisons with “truth” measurements made by the millimeter wave cloud radar (MMCR) located at NASA Atmospheric Radiation Measurement (ARM) site SGP. This radar provides highly accurate measurements of cloud base heights, cloud top heights, and cloud thickness.

Two MODIS granules were identified that had single-layers of water clouds and ice clouds during the overflight of MODIS. Color composites of the MODIS data for these scenes are shown in Figure 4 and 5 respectively along with a combination of the

automated VIIRS cloud mask and cloud top phase analyses that were ancillary data for the COP and CBH algorithms. Data in Figure 4 were collected by MODIS/Terra on 7 October 2000 at 0435 UTC while data in Figure 5 were collected on 15 November 2000 at 0440 UTC. The location of the SGP ARM site is indicated by a "star" in the color composites.

Figure 4 here.

Figure 5 here.

The color composites shown in these figures were created by assigning data in the 3.7 μm, 11.0 μm, and 12.0 μm MODIS bandpasses, i.e. Channels 20, 31, and 32, in the inverted mode (i.e. cold clouds appearing brighter than warmer clouds) to the red, green, and blue guns of the CRT respectively. This bandpass to color gun assignment causes clouds that are more optically thick in the 12 μm band, like thin cirrus clouds, to have a bluish hue since they have a lower brightness temperature in the bandpass than in the other channels. Water clouds have a pinkish appearance due to a lower brightness temperature in the 3.7 mm band, cause by the smaller emissivity in this bandpass, compared to the longer wavelengths. Clouds that appear a shade of gray have nearly the same brightness temperatures in all three bandpasses with dense cirrus appearing most bright since it is colder than the water cloud tops. A darker shade of gray seems to be present in clouds classified as mixed ice an water phase by the VIIRS cloud top phase algorithm. Most importantly, the cloud phase passed to the COP and CBH algorithms appears to be correct for both data sets. (Differences in cloud top phase legends results from using two different cloud top phase algorithms to produce the results. The original MODIS cloud phase algorithm produced three cloud phases as shown in Figure 4 while

the new VIIRS cloud phase algorithm developed by Pavalonis and Heidinger (2004) produces seven classes as shown in Figure 5.)

4.0 VIIRS CLOUD BASE HEIGHT ALGORITHM PERFORMANCE

Results from the analyses of MODIS data sets, described in the previous section, with the cloud algorithms developed for the VIIRS sensor are shown in Figure 6 and Figure 7. The first figure contains the water cloud while the second figure has results from the analysis of the ice cloud case study.

The upper left panel in Figure 6 contains cloud top heights and bases constructed from the merged minutes of the MMCR at ARM SGP site OK. Show is a time series collected between 0300 – 0600 UTC on 7 October 2000. MODIS overflew this site at 0435 UTC as indicated by the arrow. At the time of MODIS overflight, this relatively persistent and uniform cloud field had a cloud top height of slightly less than 3.5 km and a cloud base height of about 2.25 km. The cloud thickness was observed to vary between about 0.6 – 1.0 km as shown in the lower left panel of this figure. Also noted in passing that the cloud base became lower as the night progress (local midnight is 0600 UTC) and the cloud thickness increased to about 1.5 km.

Based upon the cloud mask and cloud top phase analysis shown in Figure 4, the VIIRS COP, CTP, and CBH algorithms were run on the test case. The COP algorithms produced cloud top temperatures using the approach discussed in Section 2.2 and these temperatures were converted into cloud top heights using NCEP atmospheric profiles

with an interpolation scheme contained in the CC/L algorithms. The resulting cloud top heights are shown as “blue circles” in the top right panel of Figure 4. Also shown is the NPOESS cloud top height requirement of +/- 1 km in dashed lines along with the retrieval obtained by converting MODIS cloud top pressures into cloud top height using the same interpolation scheme used with the VIIRS retrieved cloud top temperatures. While the VIIRS algorithms we at the limit of the NPOESS requirements for the cloud top height product, MODIS produced at better result in this case. The MODIS approach assumes that cloud top pressures below 700 mb are indicative of optically thick clouds; therefore, the clouds are assumed to be black bodies (Platnick et al., 2003). This approach is appealing since it bypasses the COP algorithms currently used in the VIIRS cloud module architecture shown in Figure 1 and the performance of these algorithms has not yet been fully established in degraded conditions such as regions of sunglint and the terminator orbit. Therefore, the results shown in this panel supported a decision to incorporate the MODIS approach for retrieving cloud top properties of lower-level water clouds into the VIIRS cloud top parameters (CTP) algorithm architecture. Further testing will be needed to determine when to apply the different algorithms. This additional flexibility was also included in the clustering algorithms used in the CC/L algorithms which will be discussed in a separate paper.

The VIIRS cloud base heights retrieved from the approach described in Section 2.1 on the MODIS scene shown in Figure 4 is in the lower right panel of Figure 6. Those observations most close to the satellite overflight are presented by blue circles while the NPOESS CBH data product requirement of +/- 2 km is shown by the dashed lines.

Clearly, the retrieved cloud base heights are well within the NPOESS requirements range. However, the dependence upon this product on the cloud top height product is shown by the offset of the cloud base toward larger values, e.g. as were the cloud top height retrievals shown in the upper right panel.

Perhaps most importantly, the retrieved VIIRS cloud thickness values ranged between 0.2 – 0.9 which suggests that the VIIRS algorithms are producing a realistic nighttime COP product since cloud thickness is converted cloud optical properties to geometric thickness using the parameterization shown in Equations 1 and 2 for water clouds. Therefore, a major risk associated with the retrieval of cloud base heights in nighttime VIIRS imagery appears less problematic that originally believed by the VIIRS CBH developer, even though sensitivity studies, conducted early in the NPOESS program, suggested cloud top heights would be the error source drivers in the CBH product (Hutchison, 1998).

Figure 7 contains information, organized in the same manner shown in Figure 6, for the retrieval of cloud top height, cloud base height, and cloud thickness of the ice cloud shown in Figure 5.

Upon inspection of the cloud signatures recorded by the MMCR at ARM SGP site OK, shown in the upper left panel, the reason for more relaxed NPOESS system requirements for the cloud top height product becomes evident. Both cloud top heights and cloud base heights are seen to be highly variable, in a manner consistent with observations made by Wylie (1994). In fact, even with the MMCR reports, it is difficult to determine the height of clouds actually observed by the MODIS sensor since observations shown variations on

the order of 1 km within a matter of minutes in the vertical position above the site. MODIS observations were through a slight slant path. In addition, the cloud bases are quite ragged also and vary between nearly 8-10 km during the 0300 – 0600 timeframe which a local minima in the cloud base near the time of MODIS overflight. Indeed, cloud thickness values reported by the MMCR are shown in the lower left panel to be highly variable. At precisely the time MODIS overflew the site, cloud thickness values were reported between 0.8-2.1 km; however, within minutes of this time this range had increased to between 0.5-2.3 km. Therefore, the exact heights of the cloud tops and bases are not known as precisely for this data set as they were for the water cloud case.

Pixel-level retrievals of cloud top heights are shown in the upper right panel with results from the VIIRS algorithms shown again as blue circles while those reported by the NASA algorithms in the MOD06_L2 (Terra) and MYD06_L2 (Aqua) products available through the internet, are shown as black circles. NPOESS requirements of +/- 1 km and +/- 2 km are based upon ice cloud optical thickness reports with the larger error bar associated with ice cloud optical thickness values smaller than 1.0 while the smaller error bar applied to ice clouds with larger optical thickness values. To more correctly compare VIIRS and MODIS results, the pixel-level VIIRS data were aggregated to 5 km which is the cell size of the MODIS product. Arrows are used to identify these aggregated values. In general, all the VIIRS aggregated data fall within the NPOESS system requirement while some MODIS observations are reported much lower. These lower MODIS cloud top heights may be associated with the theory behind the CO2 slicing algorithm which can retrieve cloud top pressures that with errors that average 100 mb in the presence of multi-layered (thin cirrus over lower-level water) cloud systems (Menzel et al., 2002). In

this case, lower-level water clouds are observed after but not during the MODIS overflight. Again, it is not know exactly what clouds might have been in the MODIS field of view since no attempt is made to correlate the MMCR observations with the MODIS slant path data. The fact the VIIRS algorithms does not produce cloud top heights below 8 km is a source of encouragement. In the absence of the 13-14 μm channels in the MODIS sensor, the approach to retrieving cloud top parameters taken by NASA, in using the CO_2 slicing algorithm, is not an option with the VIIRS sensor.

A comparison between VIIRS cloud thickness values and those reported by the MMCR are shown in the lower-left panel with the MMCR and VIIRS retrieved cloud bases in the lower-right panel. It is obvious that both are ranging widely at or near MODIS overflight time. VIIRS cloud thickness values range between 0.8-1.8 while MMCR observations, as noted above, range somewhere between 0.5-2.3 km and 0.8-2.1 km. Using best estimates of the cloud top heights and cloud thickness values retrieved from VIIRS algorithms, the cloud base height products, shown again as blue dots in the lower-right panel, appear well within the range of NPOESS system requirements. Therefore, it is again concluded that the approach used to retrieve cloud base heights and their dependence upon the simultaneous retrieval of COP and cloud top temperatures, discussed in Section 2.2, appears to be justified.

5. FUTURE WORK

A good start has been made in the verification of the theoretical basis for the retrieval of cloud products in current MODIS and future VIIRS nighttime data. Initial results are encouraging but more verification testing is planned using a combination of global

synthetic data and global MODIS data sets. The approach taken to create global, synthetic data sets has been discussed (Grano et al., 2004) and these data are invaluable for establishing the performance of cloud algorithms and data products retrieved with them. However, variations of this approach are needed to create structured cloud scenes of synthetic cloud data. Good progress has been made in assessing the accuracy of existing radiative transfer codes for this task and making needed corrections (Ou et al., 2005). In the meantime, additional testing is planned with organizations prepared to analyze global data sets of MODIS data and already assisting in the analysis of these data with the VIIRS cloud mask algorithms. They included NOAA National Environmental Satellite Data and Information Service (NESDIS) located at the University of Wisconsin (UW), the Cooperative Institute for Meteorological Satellite Systems (CIMSS) at UW, and The Aerospace Corporation in Omaha, NE (Hutchison et al., 2005 – in press).

As mentioned previously, the VIIRS cloud top parameter algorithms will be modified to include the MODIS approach to retrieve cloud top temperature, heights, and pressures along with the current approach described in Section 2.2 above. The logic to determine when each algorithm is used will be delayed until the algorithm suite has been more fully tested on the data sets described in the preceding paragraph. However, the approach used by NASA, based upon the assumption that clouds are black bodies, will not be applied to clouds classified as ice by the cloud top phase algorithm. Additional research is needed to determine the errors associated with applying this logic in cloud fields classified to be mixed phase, i.e. consisting of ice and water particles of different concentrations.

An assumption is made in the cloud base height algorithms that liquid water content or ice water content is constant with cloud thickness which was noted earlier in the paper and others (Hutchison 2002) to be a weakness of the approach, for all but stratiform-type clouds. Further work should be done to observe vertical profiles of these quantities, e.g. as a function of cloud type through remote sensing or in situ measurements, to better understand the impact of this assumption. If errors caused by this assumption are not too large, it could be possible to extend the value of the VIIRS cloud base height algorithms to more convective clouds using water content or ice water content retrieved from microwave imagery.

The original formulation of the VIIRS CBH algorithms were designed to complement another approach to retrieve cloud base heights to apply with microwave data (Wilheit and Hutchison, 2000). Each of these approaches has limitations that make it mandatory that a final CBH product use information from both data sources. In addition, the best approach should include the use of conventional weather observations, e.g. surface reports, where available and an architecture for this multi-source cloud base algorithm has been proposed. (See Figure 4 in Hutchison, 2002.) Results obtained from the data presented in the paper suggest yet another important application for the VIIRS CBH algorithms. Based upon case studies present herein, it appears possible to use this approach with surface observations to improve specification of cloud top heights. Thus, in heavily populated areas, where such reports are common, it might be possible to obtain improved 3-dimensional cloud fields that are needed to provide improved actinic fluxes for the chemistry models that support air quality managers.

Finally, the VIIRS cloud phase algorithm has been demonstrated to accurately detect instances when both ice and lower level water clouds (Pavolonis and Heidinger, 2004). However, no other cloud algorithm is known by these authors to be capable of exploiting this information. The VIIRS cloud base and cloud optical property algorithms assume that a single cloud layer is present in any given pixel. When this is not the case, results are expected to become degraded. Further research is needed to better understand how best to exploit the presence of multi-level clouds, e.g. in the COP CTP, CC/L, and CBH algorithms.

6. CONCLUSIONS

Evidence presented in this paper suggests that the retrieval approach used in the VIIRS cloud module will provide cloud base height data products that will satisfy NPOESS system requirements. Since COP data products are retrieved by NASA with MODIS data only during daytime conditions, the absence of a demonstration that COP algorithms retrieve accurately cloud optical thickness and cloud particle sizes, especially for water clouds during nighttime conditions, constituted the largest uncertainty in the performance of the VIIRS cloud base height algorithms. Test cases selected for this study and retrieved cloud thickness values from these data have shown clearly that the VIIRS COP algorithms produce reliable products in MODIS nighttime data. In addition, the current VIIRS cloud top height algorithms appear to produce products that meet these same system requirements, even before the additional robustness is provided adding the NASA approach for selective use with nighttime water clouds. Therefore, it is concluded that the

VIIRS cloud base height data products will meet the performance requirements established in the NPOESS system requirements documents.

7. ACKNOWLEDGMENTS

We acknowledge the support and encouragement received from leadership at NGST, UCLA, and the NPOESS IPO.

8. REFERENCES

Grano, V., Scalione, T., Emch, P., Agraveante, H., Hauss, B., Jackson, J., Mills, S., Samec, T. and M Shoucri, 2004: End-to-end performance assessment of the National Polar-orbiting Operational Environmental Satellite System environmental data records, Conf. On Weather and Environmental Satellites, Proceedings of SPIE, 5549.

Hutchison, K. D., 2002: "The Retrieval of Cloud Base Heights from MODIS and 3-Dimensional Cloud Fields from NASA's EOS Aqua Mission," International Journal of Remote Sensing. **23**, 5247-5263.

Hutchison, K. D., Roskovensky, J., Jackson, J., Heidinger, A., Pavolonis, A., Frey, R., and T. Kopp (in press): Automated cloud detection and typing of data collected by the Visible Infrared Imager Radiometer Suite (VIIRS).

Hutchison, K., 1998: VIIRS Cloud Base Height Algorithm Theoretical Basis Document, Version 1.0, Raytheon Information Technology and Scientific Services, pp. 47. (Note: Version 5 available at http://www.ipo.noaa.gov/library_NPOESS.html)

King, M. D., and Coauthors, 2003: Cloud and aerosol properties, precipitable water, and profiles of temperature and humidity from MODIS, IEEE Transactions in Geoscience and Remote Sensing, **41,** 442–458.

Liou, K-N., 1992: Radiation and Cloud Processes in the Atmosphere, Oxford press, pp 487.

Martin, G. M., Johnson, D. W. and A. Spice, 1994: The measurement and parameterization of effective radius of droplets in warm stratocumulus clouds, Journal of Atmospheric Science, **51**, 1823-1842.

Menzel W. P., Baum, B. A., Strabala, K. I. and R. A. Frey, 2002: Cloud Top Properties and Cloud Phase Algorithm Theoretical Basis Document, MODIS ATBD Reference Number: ATBD-MOD-04, pp 61.

Nakajima T. and M. D. King, 1990: Determination of the optical-thickness and effective particle radius of clouds from reflected solar-radiation measurements. 1. Theory, J. Atmos. Sci. **47**, 1878-1893.

Ou, S. C., Liou, K. N., Takano, T., Wong, E., Hutchison, K. D., and T. Samec, 2005: Comparison of the UCLA-LBLE Radiative Transfer Model and MODTRAN for Accuracy Assessment of NPOESS-VIIRS Cloud algorithms, Submitted to Applied Optics.

Ou, S. C., Takano, Y., Liou, K. N., Higgins, G. J., George, A. and R. Slonaker, 2003: Remote sensing of cirrus cloud optical thickness and effective particle size for the National Polar-orbiting Operational Environmental Satellite System Visible/Infrared Imager Radiometer Suite: sensitivity to instrument noise and uncertainties in environmental parameters, Applied Optics, **42**, 7202-7204.

Ou, S. C., Liou, K.-N., Takano, Y., VIIRS Cloud Optical Properties Algorithm Theoretical Basis Document, Raytheon Information Technology and Scientific Services, pp. 196. (Note: Available online at http://www.ipo.noaa.gov/library_NPOESS.html)

Ou S. C., Liou K.-N., Takano Y., Rao N. X., Fu Q., Heymsfield A. J., Miloshevich L.M., Baum B.and S. A. Kinne, 1995: Remote sounding of cirrus cloud optical depths and ice crystal sizes from AVHRR data: Verification using FIRE II IFO measurements, J. Atm. Sci. **52**, 4143-4158.

Ou, S. C., Liou, K-N., Gooch, W. M. and Y. Takano, 1993: Remote sensing of cirrus cloud parameters using advanced very-high resolution radiometer 3.7 and 10.9 micron channels, Appl. Opt., **32**, 2171-2180.

Pavolinis, M. J. and A. K. Heidinger, 2004: Daytime cloud overlap detection from AVHRR and VIIRS, Journal of Applied Meteorology, **43**, 762-778

Platnick S., King M. D., Ackerman S. A., Menzel W. P., Baum B. A., Riedi J. C., Frey R. A., 2003: The MODIS cloud products: Algorithms and examples from Terra, IEEE Transactions on Geoscience and Remote Sensing, 41, 459-473.

Slingo, A., Nicholls, S. and J. Schmetz, 1982: Aircraft observations of marine stratocumulus during JASIN, Quarterly Journal of the Royal Meteorological Society, **108**, 833-856.

Wilheit, T. T. and K. D. Hutchison, 2000: "Retrieval of Cloud Base Heights from Passive Microwave and Cloud Top Temperature Data," IEEE Transactions on Geoscience and Remote Sensing, **38**, 1253-1259.

Wylie, D. P., Menzel, W. P., Woolf, H. M. and K. I. Strabala, 1994: Four years of global cirrus cloud statistics using HIRS, Journal of Climate, 7, 1973-1986.

Figure Captions

Figure 1. Architecture of the VIIRS cloud algorithms.

Figure 2. Geometry for retrieval of cloud base height using cloud top height along with cloud optical properties the obtain cloud thickness (Hutchison, 2002).

Figure 3. Architecture for the retrieval of ice cloud microphysical properties from VIIRS data during daytime conditions and VIIRS data during nighttime. T_c, and D_e are cloud top temperature and ice crystal diameter.

Figure 4. Color composite of MODIS imagery (0435 UTC on 7 October 2000) shows clouds over ARM SGP Site, OK (left) along with VIIRS automated cloud mask and cloud top phase analyses (right).

Figure 5. Color composite of MODIS imagery (0440 UTC on 15 November 2000) shows clouds over ARM SGP Site, OK (left) along with VIIRS automated cloud mask and cloud top phase analyses (right).

Figure 6. MMCR measurements for ARM SGP site OK on 7 October 2000 (upper left) compared to VIIRS and MODIS cloud top heights (upper right), VIIRS cloud thickness compared to MMCR measurements (lower left) and VIIRS retrieved cloud base heights (lower right).

Figure 7. MMCR measurements are ARM SGP site OK (upper left) on 15 November 2000 compared to VIIRS and MODIS cloud top heights (upper right), VIIRS cloud thickness compared to MMCR measurements (lower left) and VIIRS retrieved cloud base heights (lower right).

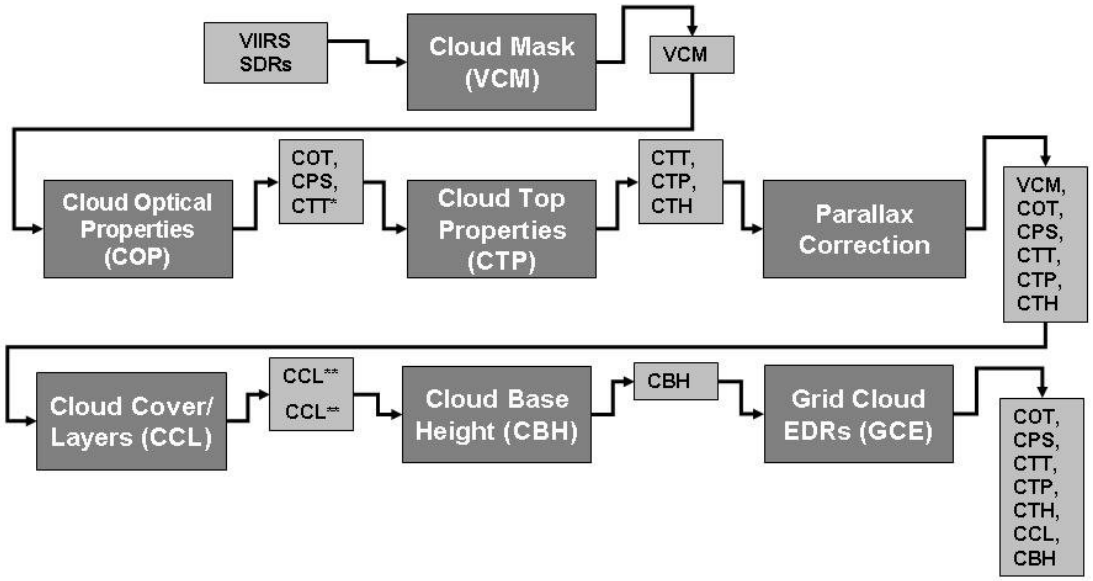

Figure 1. Architecture of the VIIRS cloud algorithms.

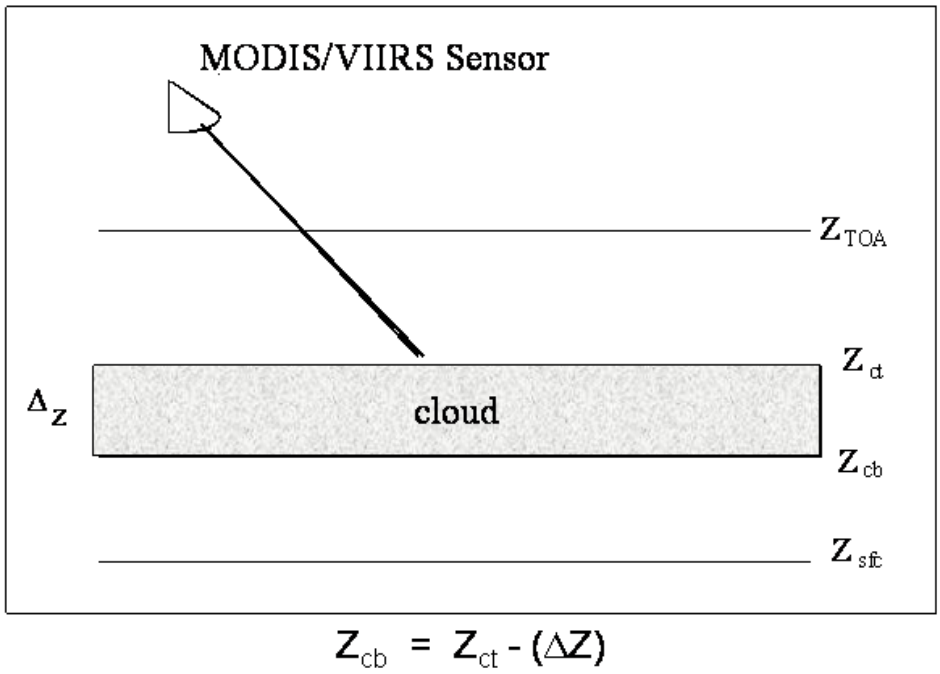

Figure 2. Geometry for retrieval of cloud base height using cloud top height along with cloud optical properties the obtain cloud thickness (Hutchison, 2002).

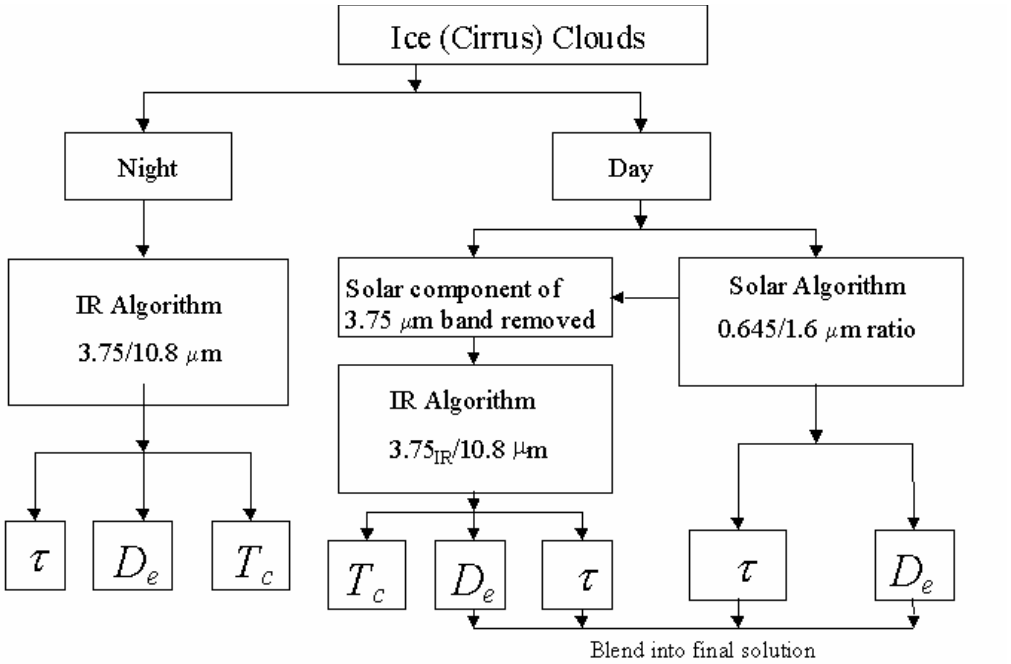

Figure 3. Architecture for the retrieval of ice cloud microphysical properties from VIIRS data during daytime conditions and VIIRS data during nighttime. T_c, and D_e are cloud top temperature and ice crystal diameter .

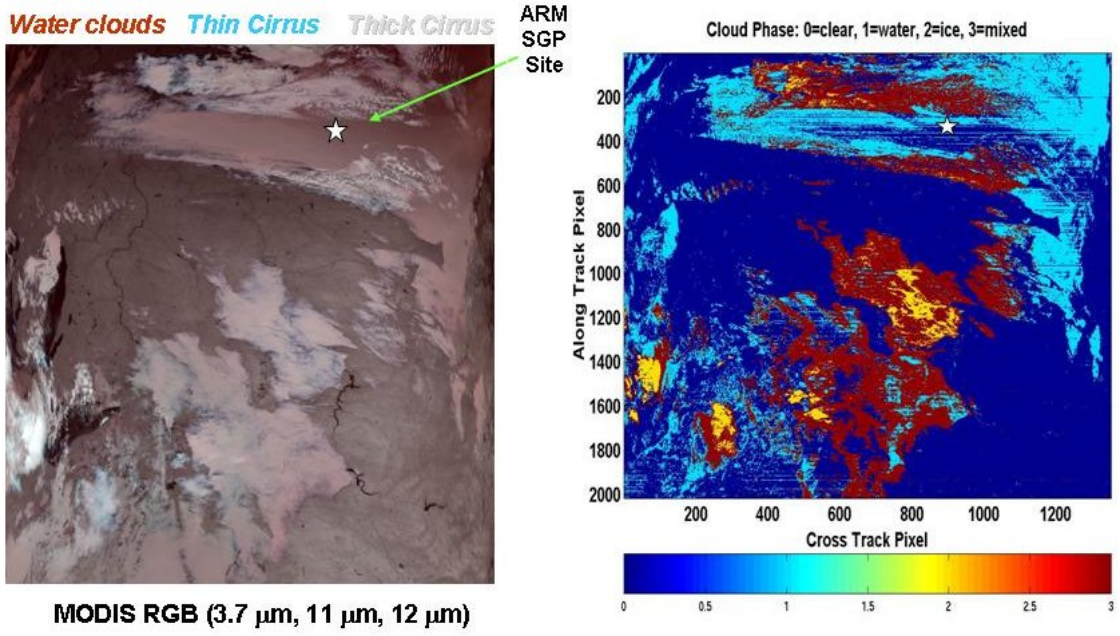

Figure 4. Color composite of MODIS imagery (0435 UTC on 7 October 2000) shows clouds over ARM SGP Site, OK (left) along with VIIRS automated cloud mask and cloud top phase analyses (right).

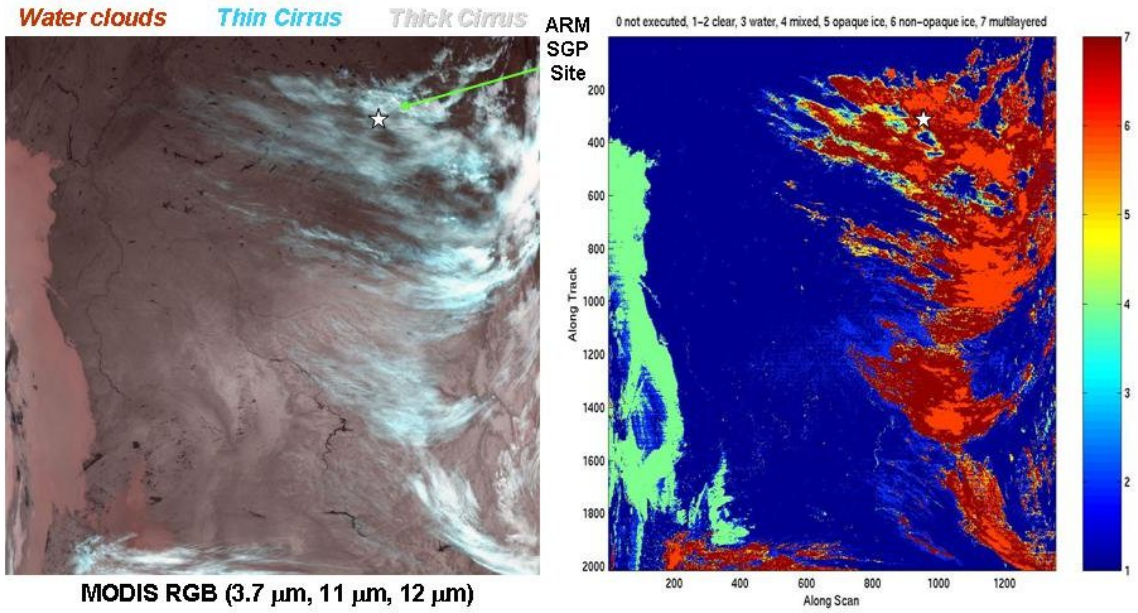

Figure 5. Color composite of MODIS imagery (0440 UTC on 15 November 2000) shows clouds over ARM SGP Site, OK (left) along with VIIRS automated cloud mask and cloud top phase analyses (right).

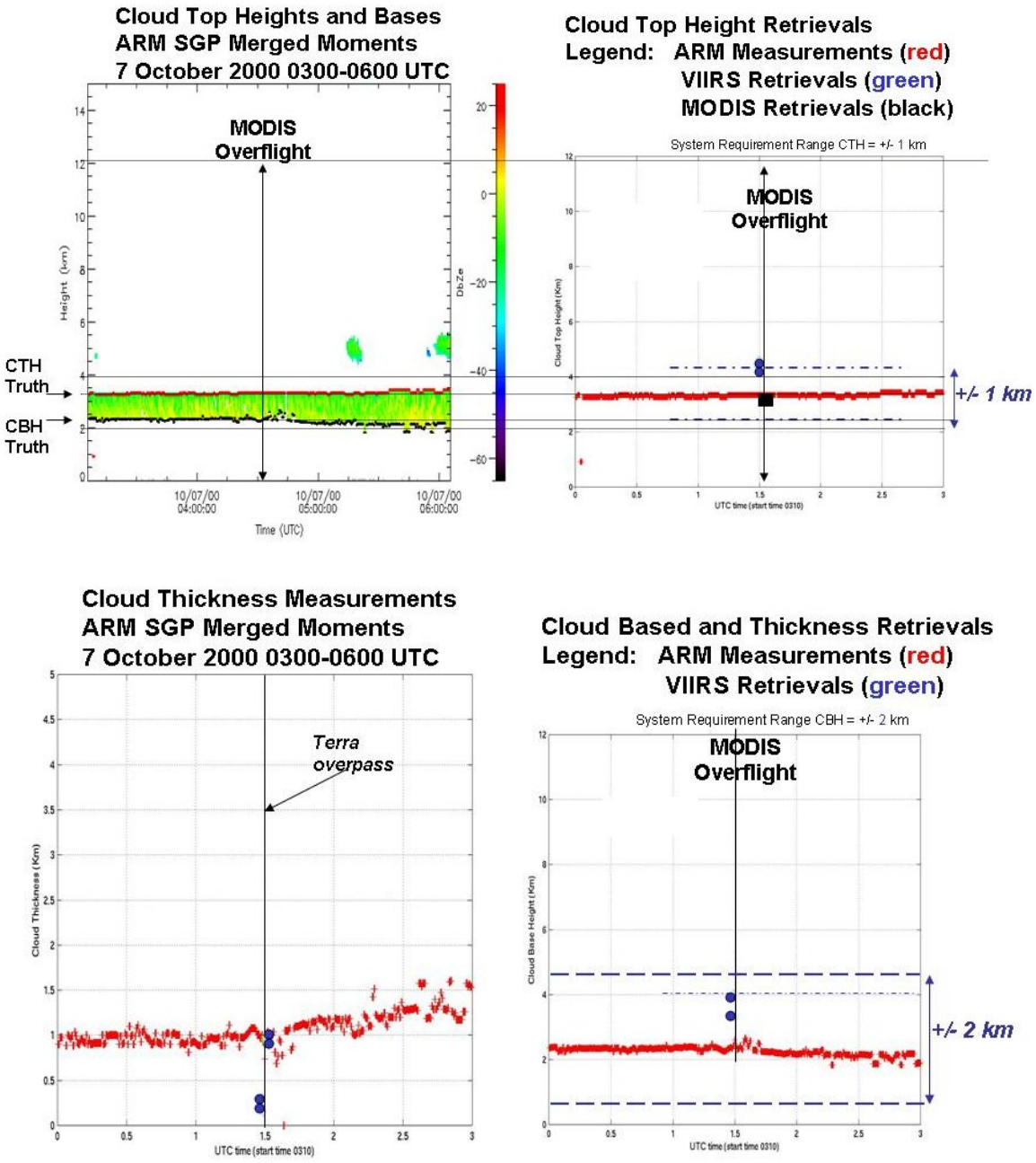

Figure 6. MMCR measurements for ARM SGP site OK on 7 October 2000 (upper left) compared to VIIRS and MODIS cloud top heights (upper right), VIIRS cloud thickness compared to MMCR measurements (lower left) and VIIRS retrieved cloud base heights (lower right).

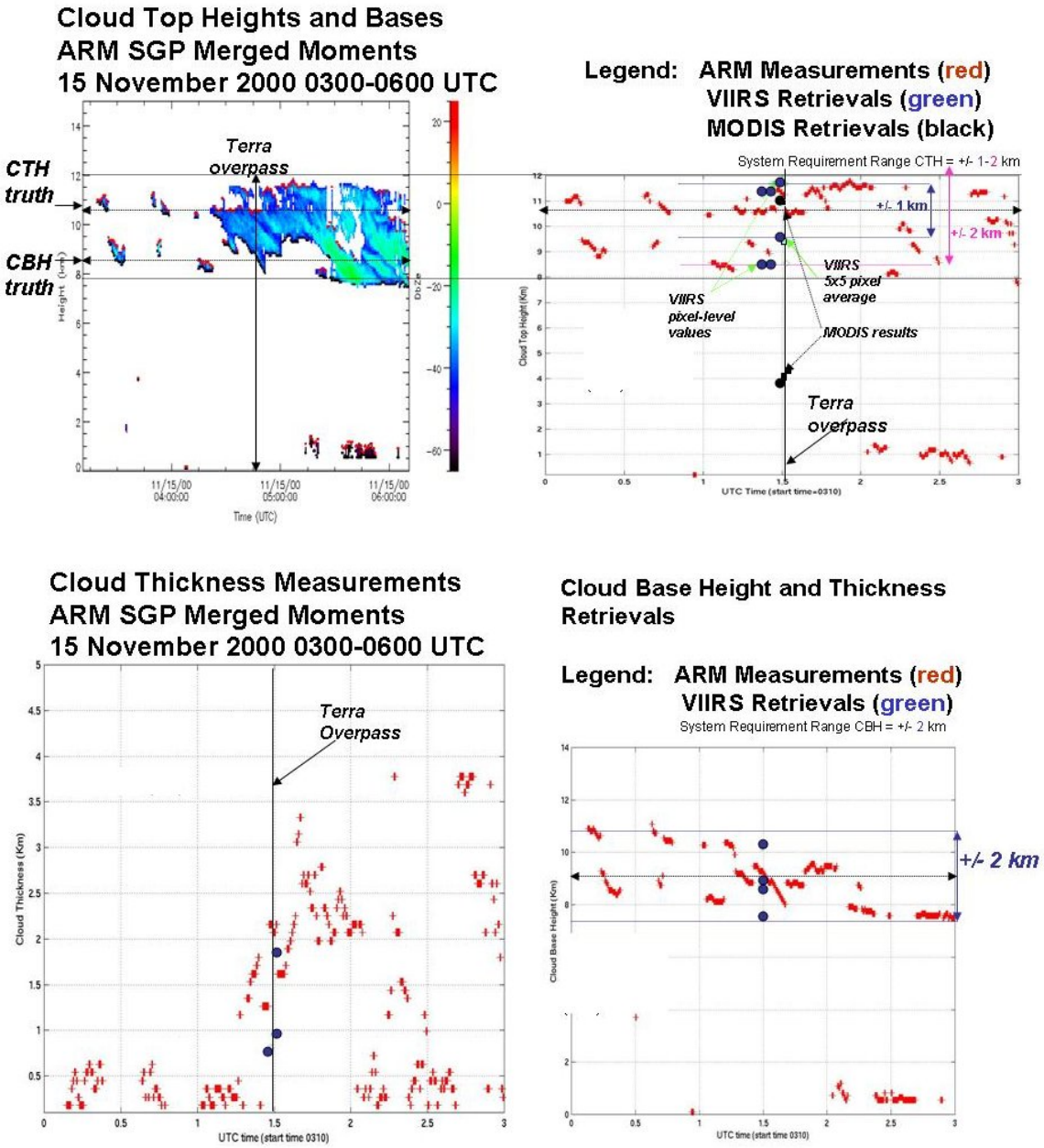

Figure 7. MMCR measurements are ARM SGP site OK (upper left) on 15 November 2000 compared to VIIRS and MODIS cloud top heights (upper right), VIIRS cloud thickness compared to MMCR measurements (lower left) and VIIRS retrieved cloud base heights (lower right).